Brain, Behavior, and Immunity 89 (2020) 118–132

Contents lists available at ScienceDirect

Brain, Behavior, and Immunity

journal homepage: www.elsevier.com/locate/ybrbi

Sleep loss disrupts pericyte-brain endothelial cell interactions impairing blood-brain barrier function

Fernanda Medina-Flores[a,b], Gabriela Hurtado-Alvarado[a], Arturo Contis-Montes de Oca[c], Stefanie Paola López-Cervantes[b,d], Mina Konigsberg[d], Maria A. Deli[e,f], Beatriz Gómez-González[a,*]

[a] Area of Neurosciences, Dept. Biology of Reproduction, CBS, Universidad Autónoma Metropolitana, Unidad Iztapalapa, Mexico City, Mexico
[b] Posgrado en Biología Experimental, Universidad Autónoma Metropolitana, Unidad Iztapalapa, Mexico City, Mexico
[c] Universidad Nacional Autónoma de México (UNAM), Facultad de Estudios Superiores (FES) Iztacala, Optometría, Mexico
[d] Laboratorio de Bioenergética y Envejecimiento Celular, Dept. Health Sciences, Universidad Autónoma Metropolitana, Unidad Iztapalapa, Mexico D.F., Mexico
[e] Institute of Biophysics, Biological Research Centre, Szeged, Hungary
[f] Department of Cell Biology and Molecular Medicine, University of Szeged, Szeged, Hungary

ARTICLE INFO

Keywords:
Blood-brain barrier
Brain endothelial cells
Connexin 43
PDGFR-β
Pericytes
Sleep loss
Tight junctions

ABSTRACT

Sleep loss in the rat increases blood-brain barrier permeability to circulating molecules by disrupting inter-endothelial tight junctions. Despite the description of the ultrastructure of cerebral microvessels and the evidence of an apparent pericyte detachment from capillary wall in sleep restricted rats the effect of sleep loss on pericytes is unknown. Here we characterized the interactions between pericytes and brain endothelial cells after sleep loss using male Wistar rats. Animals were sleep-restricted 20 h daily with 4 h sleep recovery for 10 days. At the end of the sleep restriction, brain microvessels (MVs) were isolated from cerebral cortex and hippocampus and processed for Western blot and immunocytochemistry to evaluate markers of pericyte-endothelial cell interaction (connexin 43, PDGFR-β), tight junction proteins, and proinflammatory mediator proteins (MMP9, A_{2A} adenosine receptor, CD73, NFκB). Sleep restriction reduced PDGFR-β and connexin 43 expression in MVs; in addition, scanning electron microscopy micrographs showed that pericytes were detached from capillary walls, but did not undergo apoptosis (as depicted by a reduced active caspase-3 expression). Sleep restriction also decreased tight junction protein expression in MVs and increased BBB permeability to low- and high-molecular weight tracers in *in vivo* permeability assays. Those alterations seemed to depend on a low-grade inflammatory status as reflected by the increased expression of phosphorylated NFκB and A_{2A} adenosine receptor in brain endothelial cells from the sleep-restricted rats. Our data show that pericyte-brain endothelial cell interaction is altered by sleep restriction; this evidence is essential to understand the role of sleep in regulating blood-brain barrier function.

1. Introduction

Pericytes are perivascular cells that surround the endothelium and contribute to blood-brain barrier stabilization through the induction of endothelial tight junctions and establishment of gap junctions with brain endothelial cells (Fujimoto, 1995; Armulik et al., 2010). Pericytes regulate capillary diameter, cerebral blood-flow and control the entry of immune cells to the central nervous system during angiogenesis and blood-brain barrier maturation (Armulik et al., 2005; Shimizu et al., 2008; Stark et al., 2013; Hall et al., 2014; Neuhaus et al., 2017). Reduced pericyte coverage induces microvascular defects (Benjamin et al., 1998; Tarallo et al., 2012) and blood-brain barrier dysfunction (Vates et al., 2010; Bell et al., 2010; Rustenhoven et al., 2017).

The platelet-derived growth factor receptor-β (PDGFR-β) is expressed predominantly in pericytes (Armulik et al., 2005) and its endothelium-secreted ligand, PDGF-B, has been proposed as the signaling molecule that modulates pericyte-endothelial cell crosstalk (Lebrin et al., 2010; Armulik et al., 2011). Animal models with impaired PDGFB-PDGFR-β signaling pathway present brain microvascular dysfunction (Villaseñor et al., 2017; Arango-Lievano et al., 2018) and perinatal death (Leveen et al., 1994). In addition, monocultures of endothelial cells present lower transendothelial electrical resistance (TEER) and higher permeability to low- and large-molecular weight tracers than co-cultures of brain endothelial cells and pericytes

* Corresponding author at: Area of Neurosciences, Dept. Biology of Reproduction, CBS, Universidad Autónoma Metropolitana, Unidad Iztapalapa, Av. San Rafael Atlixco No. 186, Col. Vicentina, Iztapalapa, Mexico City, 09340, Mexico.
E-mail addresses: mkf@xanum.uam.mx (M. Konigsberg), deli.maria@brc.hu (M.A. Deli), bgomezglez@gmail.com (B. Gómez-González).

https://doi.org/10.1016/j.bbi.2020.05.077
Received 3 December 2019; Received in revised form 12 April 2020; Accepted 29 May 2020
Available online 31 May 2020
0889-1591/

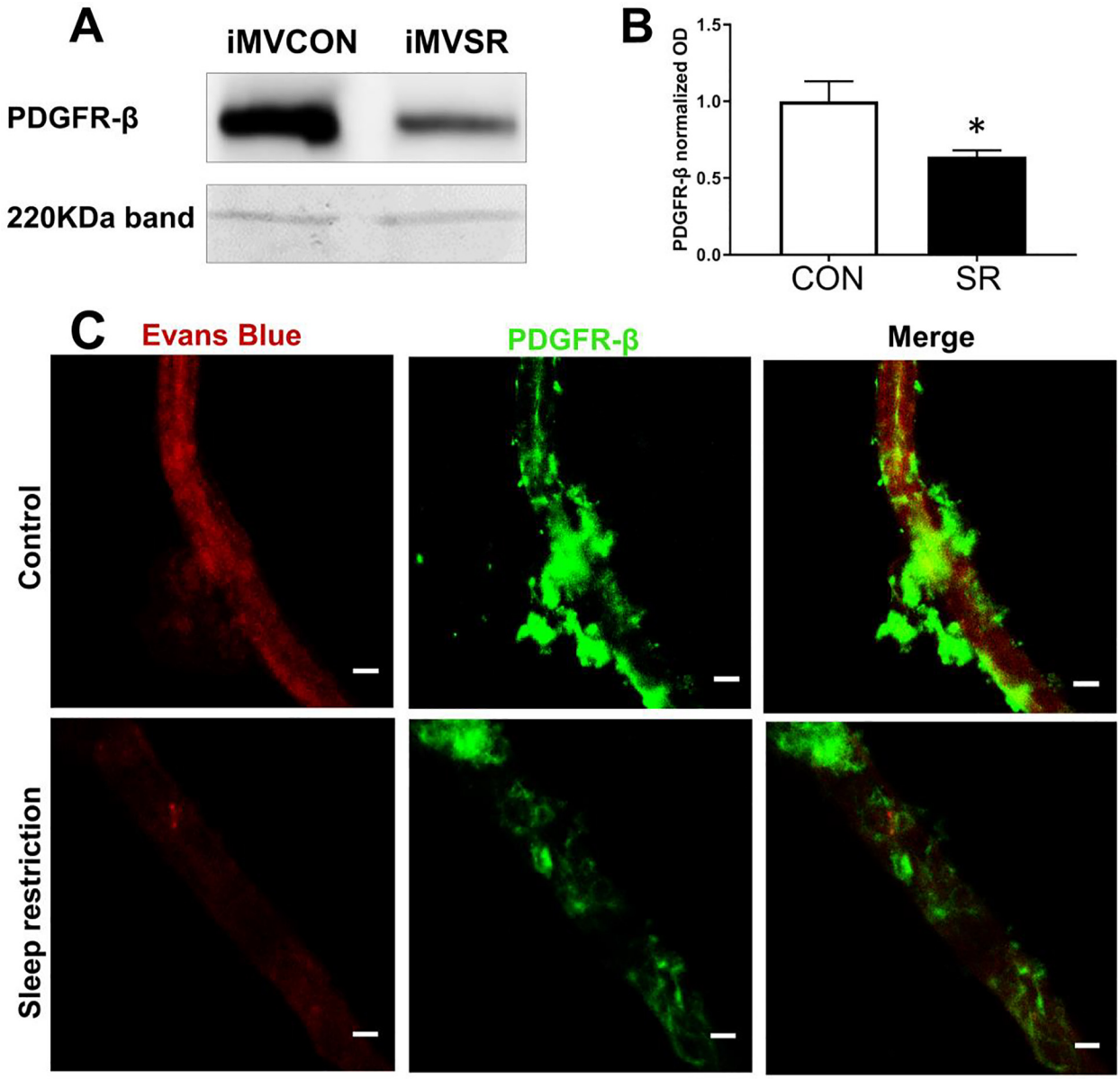

Fig. 1. Chronic sleep restriction reduces PDGFR-β expression in the cerebral cortex. A) Representative Western blot of isolated microvessels (iMV) from the control (CON, n = 6) and the sleep restricted (SR, n = 6) groups. B) Normalized levels of PDGFR-β expression in the iMV from cerebral cortex. The band of 220 KDa marked with Ponceau red was used for normalization. Samples were analyzed by duplicate in separate PVDF membranes. Mean ± standard error of the mean. *p < 0.01 as compared to the control group. C) Confocal microscopy images of iMV of CON (upper panel) and SR rats (lower panel). Note a reduced immunoreactivity of PDGFR-β (green) in SR in comparison with the CON group. Brain microvessel was marked with Evans blue (red). Scale bar: 20 μm. (For interpretation of the references to colour in this figure legend, the reader is referred to the web version of this article.)

(Hayashi et al., 2004; Nakagawa et al., 2009; Wisniewska-Kruk et al., 2012). These results underline the importance of the cell-cell interactions between brain endothelial cells and pericytes for the maintenance of the blood-brain barrier physiology.

Previous research has shown that sleep loss increases blood-brain barrier permeability to 10 kDa and 70 kDa FITC-dextrans, sodium fluorescein, and Evans blue (Gomez-Gonzalez et al., 2013; He et al., 2014; Hurtado-Alvarado et al., 2016a, 2017). Concomitant to the entry of exogenous molecules, there is a change in tight junction morphology in brain microvessels (MVs), characterized by a decrease in tight junction protein expression and the presence of wide gaps at the interendothelial junctions. In addition, our group presented ultrastructural evidence of potential pericyte detachment from the capillary wall in the hippocampus of 10-day sleep-restricted rats (Hurtado-Alvarado et al., 2018). The maintenance of the barrier properties of the blood-brain barrier seem to depend on rapid-eye movement (REM) sleep. Using the multiple platform technique for 10 days, which fully suppresses REM sleep phase and a slightly reduces non-REM sleep (around 30%), Gomez-Gonzalez et al. (2013) found large deranges in blood-brain barrier function. He et al. (2014) found that a protocol reducing 20% non-REM sleep time and greatly reducing REM sleep time (up to 80%) during 6 days of sleep restriction, induces modest changes in the barrier phenotype. In both cases chronic sleep loss induces neuroinflammation, as depicted by the increase in the expression of glial markers (eg. Iba1 and GFAP) in several brain regions (Hurtado-Alvarado et al., 2016a, 2018; Manchanda et al., 2018) and by the increase in the cyclooxygenase 2 (COX-2) mRNA in brain homogenates (He et al., 2014). Other reports have shown that sleep restriction for 21 days also increases mRNA expression of tumor necrosis factor (TNF)-α in the hippocampus (Manchanda et al., 2018).

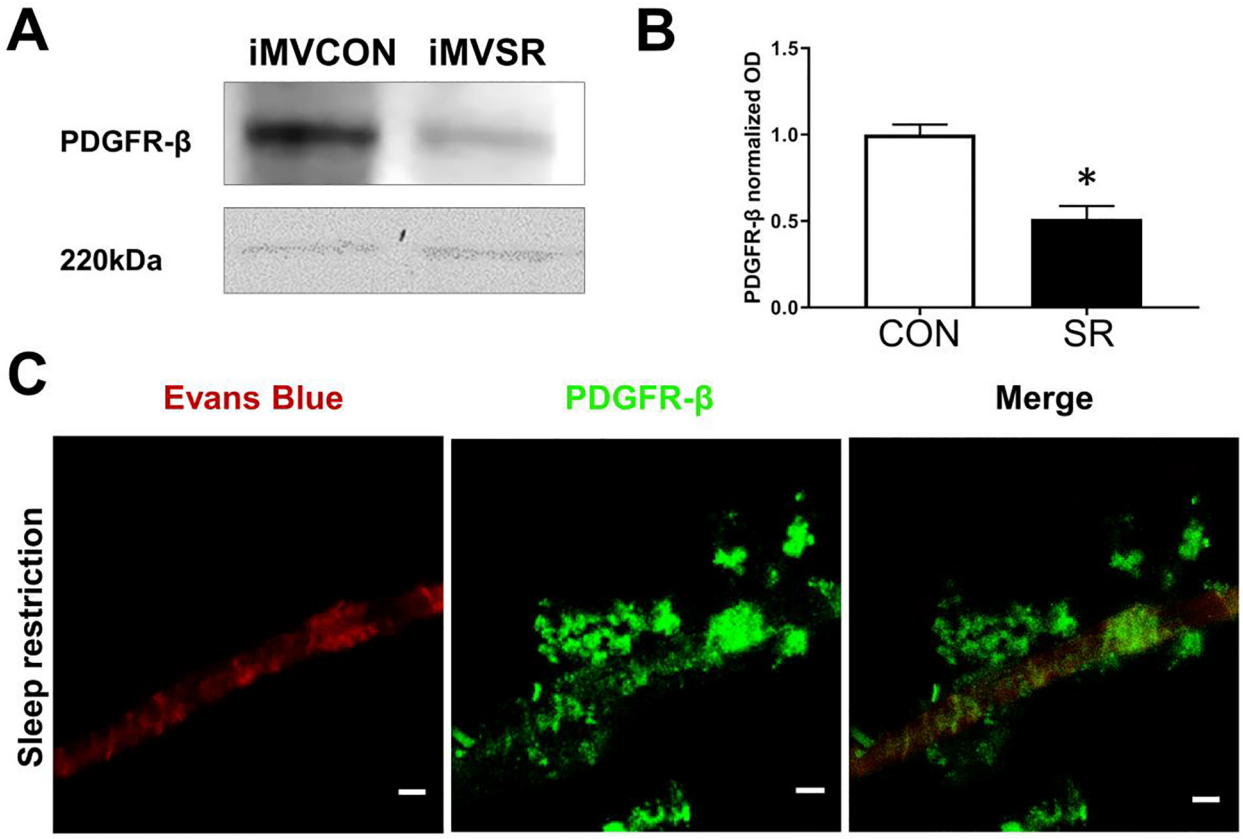

Fig. 2. Chronic sleep restriction reduces PDGFR-β expression in the hippocampus. A) Representative Western blot of the isolated microvessels (iMV) from control (CON, n = 6) and sleep restricted (SR, n = 6) groups. B) Graph depicts the normalized expression levels of PDGFR-β using a band of 220 KDa marked with Ponceau red. Samples were analyzed by duplicate in separate PVDF membranes. Mean ± standard error of the mean. *p < 0.0001 as compared to the control group. C) Confocal microscopy images of iMV from hippocampus showing PDGFR-β immunoreactivity (green) in round shaped blebbing cells in SR group. Brain microvessel was marked with Evans blue (red). Scale bar: 20 μm. (For interpretation of the references to colour in this figure legend, the reader is referred to the web version of this article.)

Both, the peripheral and the central low-grade inflammatory status during chronic sleep loss (Hurtado-Alvarado et al., 2016b), may affect the intercellular interactions between pericytes and brain endothelial cells, but the mechanisms involved in the regulation of blood-brain barrier function during sleep loss are only recently being studied. Thus, we aimed to determine the effect of sleep restriction on pericyte-brain endothelial cell interactions and their consequences on blood-brain barrier function, characterizing the inflammatory mediators that might be participating in this event.

2. Methods

2.1. Animals

Three-month old male Wistar rats were used and randomly divided in two groups: sleep restriction group (SR, n = 33) and intact control group (CON, n = 33). Animals were housed in standard conditions in our laboratory vivarium under a 12 h light-dark cycle (lights on at 11:00 am) at room temperature of 20–25 °C. Commercial rat chow and tap water were provided *ad libitum*. All experimental animal procedures were performed following the Guidelines for the Care and Use of Mammals in Neuroscience and Behavioral Research (National Research Council, 2010) and with the ARRIVE (Animal Research: Reporting *In Vivo* Experiments) guidelines (www.nc3rs.org.uk/arrive-guidelines) and were approved by the Academic Ethic Committee of the Biological Science Division of the Universidad Autónoma Metropolitana, Unidad Iztapalapa.

2.2. Sleep restriction

Rats were subjected to sleep restriction using the multiple platform technique (Gomez-Gonzalez et al., 2013). Rats were placed in an acrylic chamber (82 × 59 × 48 cm) with 7 cm diameter platforms surrounded by water for 20 h daily, with an opportunity to sleep in their home cages for the last 4 h of the light phase during 10 consecutive days (Gomez-Gonzalez et al., 2013). To reduce social stress, the animals remained in their same social group during the sleep restriction and sleep recovery periods, and to reduce restraint stress an extra platform was added to the deprivation chamber to facilitate the movement of the animals as previously reported (Gomez-Gonzalez et al., 2013). Intact controls slept *ad libitum* in their home cages during the 10 days of the experiment.

2.3. Brain microvessel isolation

Brain microvessels were isolated immediately after removing the rats from the sleep deprivation chamber at the 10th day of sleep restriction. Brain samples were also obtained from the intact control group. Animals were euthanized, their brains were removed and treated as previously reported (Nakagawa et al., 2009). The cerebral cortex and hippocampal regions were homogenized with 1 ml cold MV isolation buffer (0.3 M sucrose, 3 M HEPES, 1% BSA in PBS, pH: 7.4) and centrifuged at 1000 × *g* for 10 min at 4 °C. The supernatants were eliminated, and the pellets were resuspended in 1 ml microvessel isolation buffer, then centrifuged at 1000 × *g* for 10 min. The supernatants were obtained and centrifuged at 200 × *g* for 5 min and the pellets were

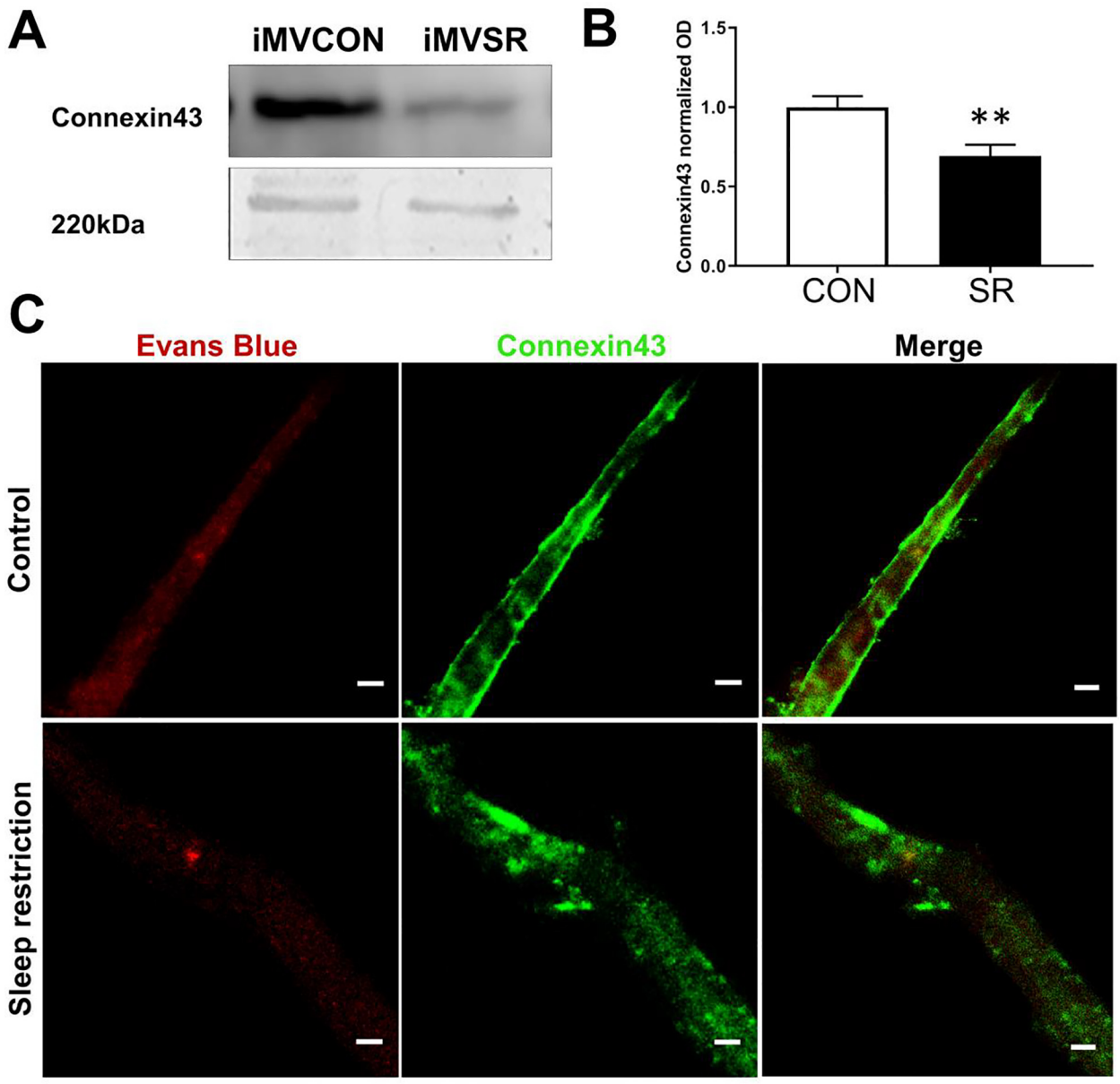

Fig. 3. Chronic sleep restriction reduces connexin 43 expression in the cerebral cortex. A) Western blot of connexin 43 in isolated brain microvessels (iMV) from sleep restriction (SR) and intact control (CON) groups. B) Graph depicts the expression levels of normalized connexin 43 using a band of 220 KDa marked with Ponceau red. Samples were analyzed by duplicate in separate PVDF membranes. Mean ± standard error of the mean. **p < 0.001 as compared to the CON group. C) Confocal microscopy images of iMV from the cerebral cortex illustrate a diminished immunoreactivity of connexin 43 (green) in SR rats (lower panel) in comparison with the CON group (upper panel). Brain microvessel was marked with Evans blue (red). Scale bar: 20 μm. (For interpretation of the references to colour in this figure legend, the reader is referred to the web version of this article.)

washed with 1 ml PBS at 100 × *g* for 2 min. The isolated brain microvessels were frozen until use. To determine that isolated brain MVs were free of neurons and astrocytes, their purity was determined by Western blot against the neuronal nuclei protein (NeuN) and the glial-acidic fibrillar protein (GFAP), as shown in Supplementary Fig. 1.

2.4. Western blot

Protein expression from isolated brain MVs was analyzed in sleep restricted and intact control groups (n = 6 *per* group). The pellet containing isolated cerebral microvessels was homogenized with 200 μl RIPA buffer containing protease inhibitors and centrifuged at 13500 rpm for 10 min at 4 °C. Protein concentration was determined with the Bradford assay (BioRad, 500-0006). The proteins (30 μg) were resolved on a 10% SDS-PAGE gel and transferred to PVDF membranes. Membranes were blocked with 5% non-fat milk in PBS containing 0.1% Triton X-100 for 2 h and incubated overnight at 4 °C with antibodies to PDGFR-β (ThermoFisher, G.290.3, 1:1000), connexin 43 (Invitrogen, 71-0700, 1:1000), active caspase-3 (BioVision, 3015-100, 1:1000), claudin-5 (Biorbyt, orb160461, 1:1000), occludin (Invitrogen, 40-4700, 1:1000), GLUT-1 (Invitrogen, PA5-16793, 1:1000), MMP9 (Abcam, ab38898, 1:1000), CD73 (Abcam, ab175396, 1:1000), A_{2A} adenosine receptor (Abcam, ab3461, 1:1000), and Phospho-NFkB p65 (Cell signaling, 3033S, 1:1000). Blots were incubated with secondary antibodies conjugated with horseradish peroxidase (1:2500 dilution) at room temperature and revealed with the chemiluminescence detection system (Amersham, RPN2232). Images were acquired using the C-DiGit image generation and analysis system (LI-COR iS image studio, version 3.1). Proteins were normalized with a 220 KDa band marked with red Ponceau.

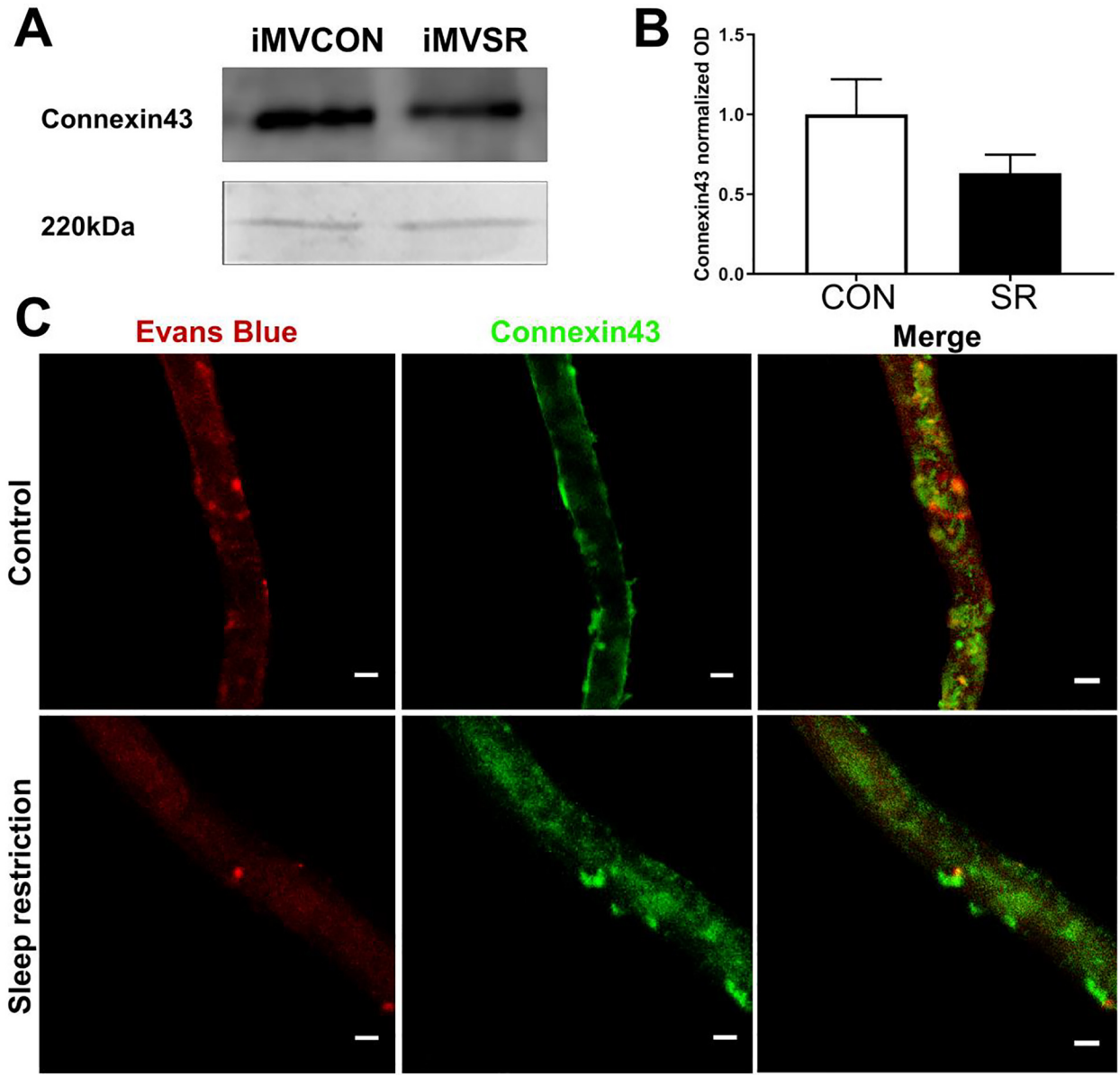

Fig. 4. Chronic sleep restriction reduces connexin 43 expression in the hippocampus. A) Western blot showing a trend toward reduction in connexin 43 expression in iMV from sleep restricted rats (SR) in comparison with the rats sleeping *ad libitum* (CON). B) Graph depicts the expression levels of normalized connexin 43 using a band of 220 KDa marked with Ponceau red. Samples were analyzed by duplicate in separate PVDF membranes. Mean ± standard error of the mean. $p > 0.05$ as compared to the control group. C) Immunofluorescent staining for connexin 43 in iMV from CON (upper panel) and SR (lower panel) groups. Note the linear expression of connexin 43 along the capillary in the iMV from the CON group and the loss of linearity in the iMV from the SR group. Brain microvessel was marked with Evans blue (red). Scale bar: 20 μm. (For interpretation of the references to colour in this figure legend, the reader is referred to the web version of this article.)

2.5. Immunofluorescence confocal microscopy

Rats from both groups, sleep restricted and intact controls (n = 5 *per* group), were ip. anesthetized with sodium pentobarbital. Evans blue dye (1 mg/ml) was ic. administrated (0.2 ml/100 g of body weight) and left to circulate for 5 min. Thereafter, animals were transcardially perfused with 0.9% saline solution. The brains were removed to isolate brain microvessels from cerebral cortex and hippocampus as previously described and resuspended in 4% paraformaldehyde 1 h and centrifuged at 13500 rpm for 10 min, the supernatant was eliminated, and the pellet was resuspended in PBS. Resuspended brain microvessels were placed on gelatinized slides and after 1 h of adherence, were rinsed with PBS containing 0.1% Triton X-100 and blocked with normal horse serum blocking solution (Vector Labs, S-2000, 1:1000) for 15 min and incubated with PDGFR-β, connexin 43, or claudin-5 antibodies under dark and humid conditions for 4 h. Slides were then incubated with the secondary antibody Alexa Fluor® 488 donkey anti-rabbit IgG (ThermoFisher, A21206, 1:250) for 4 h. The samples were mounted in ImmunoHistoMount mounting medium (Sigma, I1161-30ML). Confocal images were acquired at 488 nm excitation with a detection range of 505–535 nm and analyzed with an Axioscop 2 MOT Plus confocal fluorescence microscope (Carl Zeiss, México) with an EC Plan-Neofluar 40x/0.5 objective.

2.6. Scanning electron microscopy

Sleep-restricted and intact control rats (n = 2 *per* group) were sacrificed to isolate brain microvessels from cerebral cortex and hippocampus as described above. Isolated brain MVs were fixed with 4% paraformaldehyde and 2% glutaraldehyde for 24 h at 4 °C. Samples

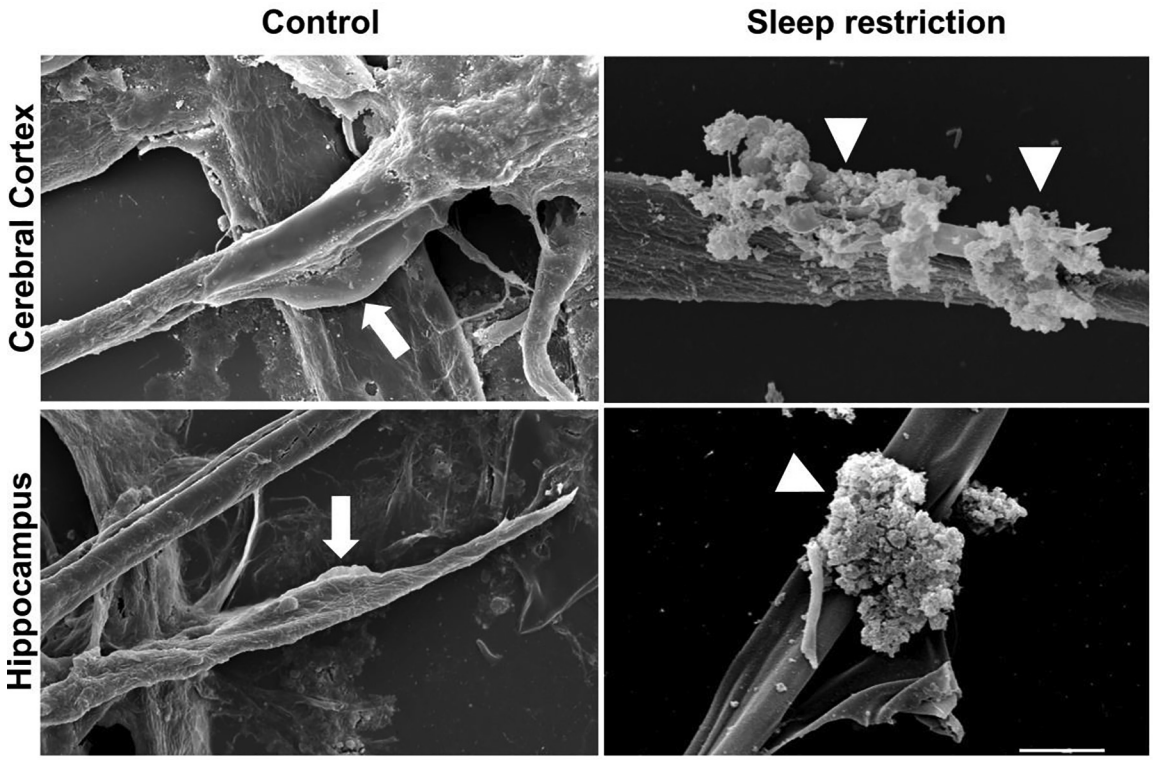

Fig. 5. Sleep loss promotes brain pericyte detachment from the capillary wall in the cerebral cortex and hippocampus. Scanning electron micrographs of isolated brain microvessels (iMV) showing pericyte detachment from the capillary wall in the cerebral cortex and hippocampus. Images also show a phenotype change in pericytes after 10 days of sleep restriction (left panels), in comparison with the group sleeping *ad libitum* (right panels) in cerebral cortex (upper panel) and hippocampus (lower panel). Note the pericyte attached to brain microvessels in the control group (arrow) and the round-shaped cells located in the vicinity of brain microvessels (arrowhead) in the sleep restricted group. Scale bar: 10 μm.

were rinsed with PBS and placed on gelatinized coverslips. The samples were post-fixed with 1% OsO_4 for 2 h at room temperature and then dehydrated in graded ethanol series. The samples were dried at the critical point in liquid CO_2, followed by gold coating. Scanning electron microscopy micrographs were acquired at 13 kV with a scanning electron microscope (JEOL JSM-5900 LV).

2.7. In vivo blood-brain barrier permeability assays

Immediately at the end of the 10th day of sleep restriction rats (n = 6 *per* group) were ip. anesthetized with sodium pentobarbital and a 0.5 cm thoracic incision was done. A cocktail containing sodium-fluorescein (Sigma-Aldrich, F6377, 10 mg/ml) and Evans blue (Sigma-Aldrich, E2129, 1 mg/ml) diluted in phosphate buffer solution was ic. administrated (0.2 ml/100 g of weight) and left to circulate for 5 min. An independent group of animals (n = 6 *per* group) received ic. administration of rhodamine 123 diluted in phosphate buffer solution (Sigma-Aldrich, 83702, 1 mg/ml, 0.2 ml/100 g of weight); rhodamine 123 was also left to circulate for 5 min. Thereafter, animals were transcardially perfused with 0.9% saline solution and the cerebral cortex and hippocampus were dissected. The samples were weighed, homogenized with cold-PBS and centrifuged at 13500 rpm/10 min at 4 °C. Supernatants were collected and methanol was added, supernatants were mixed and centrifuged at 13500 rpm/10 min at 4 °C. The supernatants were placed in a 96-well plate and absorbance values were measured in ELISA plate reader HLAB (H Reader 1) for fluorescein (485 nm excitation/535 nm emission), for Evans blue (535 nm excitation/595 nm emission), and for rhodamine 123 (535 nm excitation/595 nm emission). Each sample was quantified by duplicate. A standard curve of known concentrations of Evans blue, fluorescein and rhodamine 123 was prepared in duplicate, measured and used for the calculation of dye concentrations.

2.8. Mitochondrial oxygen consumption in brain microvessels

To evaluate the mitochondrial function at the isolated brain MVs, sleep restricted and intact control rats were euthanized, then the cerebral cortex and hippocampus were dissected and processed to isolate brain microvessels as described above. The samples were pooled for the same group of animals (n = 10 *per* group). Pools of isolated brain MVs were resuspended in 20 ml ice-cold 250 mM sucrose, 10 mM EDTA, pH = 7.4, homogenized and centrifuged at 3500 rpm for 15 min at 4 °C. The supernatant was recovered and centrifuged at 12000 rpm for 15 min at 4 °C. The supernatant was removed and the pellet of isolated mitochondria from the cerebral cortex was carefully resuspended with 1 ml of the same solution, while isolated mitochondria from hippocampus were resuspended in 300 μl of the same solution. Protein concentration was determined using the Lowry method.

Oxygen consumption was measured polarographically using a Clark type electrode in a solution containing 250 mM sucrose, 10 mM $MgCl_2$, 10 mM succinate, 10 mM H_3PO_4, 1 mM EGTA, 0.05% bovine serum albumin, pH = 7.3 and 2 mg/ml of mitochondrial protein at 37 °C. Oxygen consumption was promoted by adding 300–500 nmol of ADP (state 3 of respiration). Respiratory control was determined as oxygen consumption rate of state 3/oxygen consumption rate of state 4 (ADP was converted to ATP and respiration slowed down). Thereafter, 10 μM of carbonyl cyanide *m*-chlorophenyl hydrazine (CCCP) was added to stimulate maximal oxygen uptake.

2.9. Statistical analysis

Data obtained from control and sleep-restricted groups were compared with a one-tail *t*-student analysis. All results are presented as mean ± standard error of the mean (s.e.m). Statistically significant difference was considered at $p < 0.05$. Statistical analyses were

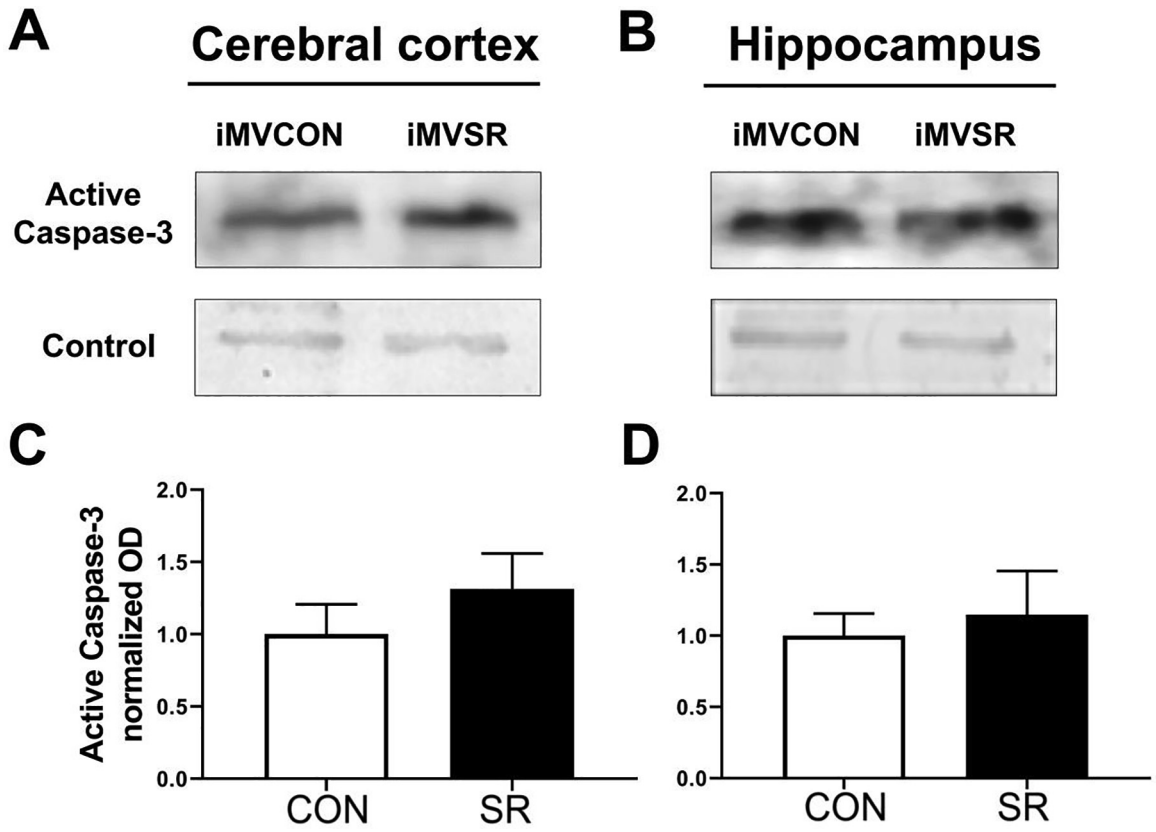

Fig. 6. Detached pericytes from sleep restricted rats did not undergo apoptosis. Representative Western blot images illustrating the expression of active caspase-3 in isolated brain microvessels (iMV) from sleep restricted (SR) and intact control (CON) groups (A, B). Graphs depict normalized expression levels of active caspase-3 using a band of 220 KDa marked with Ponceau red (C, D). Mean ± standard error of the mean. $p > 0.05$ as compared to the control group.

conducted using GraphPad Prism 8.0 software (GraphPad Software, CA, USA).

3. Results

3.1. Sleep restriction reduces pericyte-brain endothelial cell interactions

To test changes in pericyte-brain endothelial cell interactions, the expression of the proteins PDGFR-β and connexin 43 was evaluated after sleep loss. Western blot analysis showed that sleep restriction significantly decreased PDGFR-β expression in isolated brain MVs from cerebral cortex ($t = 2.623$, $p = 0.0173$) (Fig. 1A and B) and hippocampus ($t = 5.219$, $p = 0.0001$) (Fig. 2A and B). The observed changes were corroborated by confocal microscopy (Fig. 1C and C). As shown in Fig. 1C PDGFR-β immunoreactivity in the isolated microvessels from the cerebral cortex of the control group was detected surrounding capillaries with putative ramifications and the characteristic elongated pattern of a pericyte attached to the capillary wall. However, in sleep-restricted rats the PDGFR-β immunoreactivity in the isolated capillaries from the cerebral cortex was less intense and, interestingly, PDGFR-β immunostaining set apart from the capillary wall and presented a globular shape, indicating potential pericyte detachment from the capillary wall (Fig. 1C and Supplementary Fig. 2). Likely, in the hippocampus of sleep restricted rats a low immunoreactivity for PDGFR-β was observed surrounding capillaries (Fig. 2C). A 3D reconstruction of a hippocampal isolated MV showed PDGFR-β immunoreactive cells presenting a round blebbing shape, suggesting that pericytes are moving away from the capillary wall (Supplementary Fig. 3).

Sleep restriction significantly reduced the expression of connexin 43 in isolated brain MVs from cerebral cortex ($t = 1{,}038$, $p = 0.0063$) (Fig. 3); while in the hippocampus there was a trend toward reduction in the expression of connexin 43 in comparison with the control group (Fig. 4). As shown in the confocal microscopy micrograph in the control group connexin 43 immunoreactivity was continuously distributed along the capillaries and the signal intensity was higher in specific points, suggesting specific contact points between pericytes and endothelial cells in both, cerebral cortex (Fig. 3C) and hippocampus (Fig. 4C). By the contrary, in sleep restricted rats, the immunoreactivity for connexin 43 was lower and showed a discontinuous pattern along the capillaries in the isolated MV preparations from the cerebral cortex (Fig. 3C) and hippocampus (Fig. 4C).

Scanning electron microscopy showed that in the intact controls pericytes are closely attached to the capillary wall in the isolated microvessels from the cerebral cortex and hippocampus (Fig. 5). As observed in Fig. 5, pericytes from intact controls seem embedded in the same basal lamina as the endothelial cells (arrow). In the isolated MVs from the cerebral cortex and hippocampus of the sleep restricted animals round shaped blebbing cells were observed in the proximity of the capillary wall. This is consistent with the immunostaining pattern for PDGFR-β observed in confocal microscopy images. Given the high prevalence of blebbing cells in the MVs from SR group we tested whether SR induced pericyte apoptosis. As shown in Fig. 6, intact control and SR groups presented the same active caspase 3 expression levels in the cerebral cortex ($t = 0.9812$, $p = 0.3821$) and hippocampus ($t = 0.4298$, $p = 0.6895$), indicating that despite the blebbing appearance of pericytes, they are not undergoing apoptosis, but instead they appear to acquire an activated state.

3.2. The disruption of pericyte-endothelial cell interactions is associated with increased blood-brain barrier permeability

The function of the blood-brain barrier was evaluated through in

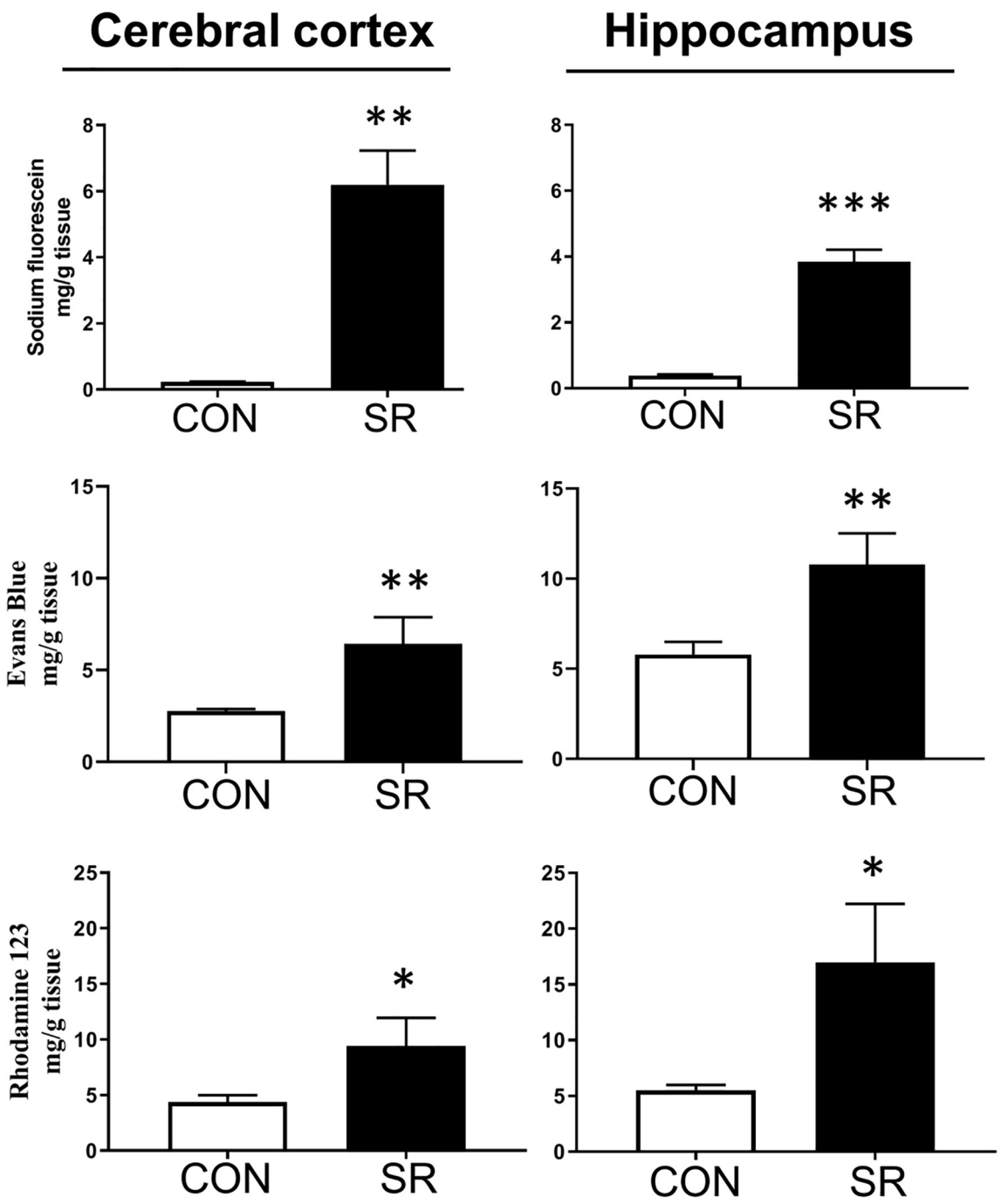

Fig. 7. Chronic sleep restriction increases blood-brain barrier permeability. Graphs depict the blood brain barrier permeability to sodium-fluorescein (upper panel), Evans blue (middle panel), and rhodamine 123 (lower panel) in the cerebral cortex and hippocampus of the intact control (CON) and sleep restricted (SR) groups. Quantification was performed by duplicate for each sample. Mean ± standard error of the mean. *$p < 0.01$, **$p < 0.001$; ***$p < 0.0001$ as compared to the CON.

vivo permeability assays with Evans blue, sodium-fluorescein and rhodamine 123 tracers. As it is shown in Fig. 7 intact controls presented low blood-brain barrier permeability to fluorescein, Evans blue and rhodamine 123 in the cerebral cortex and hippocampus. Sleep restriction significantly increased fluorescein in both brain regions, cerebral cortex ($t = 3.096$, $p = 0.0044$) and hippocampus ($t = 2.157$, $p = 0.0007$), as compared to the intact controls. The cerebral cortex ($t = 4.375$, $p = 0.0060$) and hippocampus ($t = 4.626$, $p = 0.0049$) of sleep restricted rats also presented a significant increase in blood-brain barrier permeability to Evans blue with respect to the control group. Rhodamine 123 was used to test the effects of sleep loss on the function of the P-glycoprotein efflux pump; as it is shown in Fig. 7 the cerebral cortex ($t = 1.949$, $p = 0.0436$) and hippocampus ($t = 2.184$, $p = 0.0303$) showed a significantly augmented blood-brain barrier permeability to rhodamine 123 *versus* the intact control group, indicating a decrease in pump function.

3.3. Chronic sleep restriction does not alter the metabolic activity of isolated brain microvessels

To test whether sleep loss modified metabolic activity in isolated brain MVs GLUT-1 protein expression and an oximetry assay in isolated

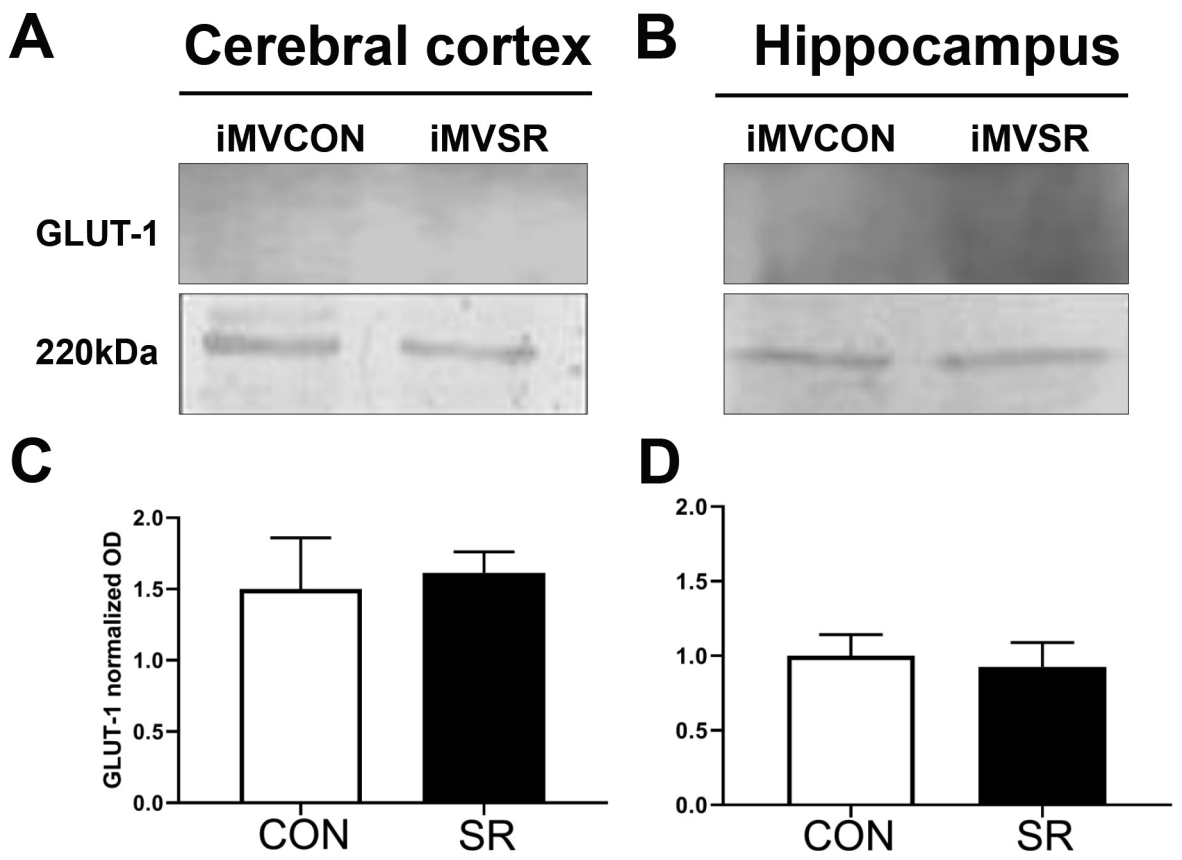

Fig. 8. Chronic sleep restriction does not alter metabolic activity in isolated brain microvessels. A, B) Western blot images illustrate the expression of GLUT-1 in isolated brain microvessels (iMV) from sleep restricted (SR) and intact control (CON) groups. C, D) Graphs depict normalized expression levels of GLUT-1 using a band of 220 KDa marked with Ponceau red. Samples were evaluated by duplicate in separate PVDF membranes. Mean ± standard error of the mean. $p > 0.05$ as compared to the control group.

Table 1
Oximetry in isolated mitochondria from the cerebral cortex brain microvessels.

Oxygen consumption	CON	SR
State 3	198 ng atom O_2/min	222 atom O_2/min
State 4	156 ng atom O_2/min	180 atom O_2/min
Respiratory Control	1.3	1.23

mitochondria were performed. As it is shown in Fig. 8, the expression of GLUT-1 transporter in isolated brain microvessels was similar in the cerebral cortex (Fig. 8A) and hippocampus (Fig. 8B) of both groups, intact control and sleep restricted ($p > 0.05$). The respiratory control was calculated from oxygen consumption experiments, using succinate as substrate to determine the mitochondrial function from isolated brain MVs. As it is shown in Table 1, the respiratory control was similar in the sleep restricted and intact control groups.

Table shows the mitochondria respiratory control of isolated brain microvessels from the cerebral cortex in the sleep restricted (SR) and intact control (CON) groups. Mean ± standard error of the mean. Data were obtained from pooled samples of $n = 10$ rats *per* each group.

3.4. The disruption of endothelial cell-pericyte interactions is associated with decreased expression of tight junction proteins

Sleep restriction modified the expression levels of endothelial tight junction proteins. Isolated brain MVs from the cerebral cortex of sleep restricted rats presented a decreased expression of claudin-5 ($t = 3.369$, $p = 0.0276$) (Fig. 9A and C); but in the hippocampal isolated MVs, normal expression of claudin-5 was observed ($p = 0.9275$ as compared to the intact controls) (Fig. 9B and D). Confocal microscopy imaging (Fig. 9E and F) showed that in both brain regions, isolated MVs from SR group showed a discontinuous staining pattern to claudin-5, but in the cerebral cortex there was also a reduced claudin-5 immunoreactivity (Fig. 9E). As it is shown in Fig. 10, the expression of occludin significantly decreased in the isolated MVs from the hippocampus of the sleep restricted group as compared to the control group ($t = 1,918$, $p = 0.0305$). However, in the cerebral cortex the occludin expression levels were similar in both groups ($p = 0.1973$). Fig. 11 shows that the decrease in tight junction protein expression was concurrent with an increased expression of MMP-9 in the isolated MVs from the cerebral cortex ($t = 2.752$, $p = 0.0131$) and hippocampus ($t = 2.452$, $p = 0.0341$) of sleep restricted rats.

3.5. Sleep loss-related low-grade inflammatory status may participate in the disruption of pericyte-endothelial cell interactions

Sleep restriction triggered a low-grade inflammatory status in the cerebral cortex and hippocampus, however the signaling pathways differ between both brain regions. In the cerebral cortex an increased expression of phosphorylated NFκB ($t = 6.758$, $p = 0.0212$) was found in the isolated MVs from the sleep restricted group as compared with the control group, despite equal levels in the expression of total NFκB (Fig. 12A and C). No differences were observed in phospho-NFκB expression in the hippocampus of sleep restricted rats with respect to the control group ($p = 0.6073$) (Fig. 12B and D). In contrast, in the isolated brain MVs from the hippocampus of sleep restricted rats an increased expression of A_{2A} adenosine receptor ($t = 2.483$, $p = 0.0324$) was found as compared with the control group (Fig. 12A and C). In the cerebral cortex, the expression of the A_{2A} adenosine receptor did not change after chronic sleep restriction ($p = 0.3941$). The expression

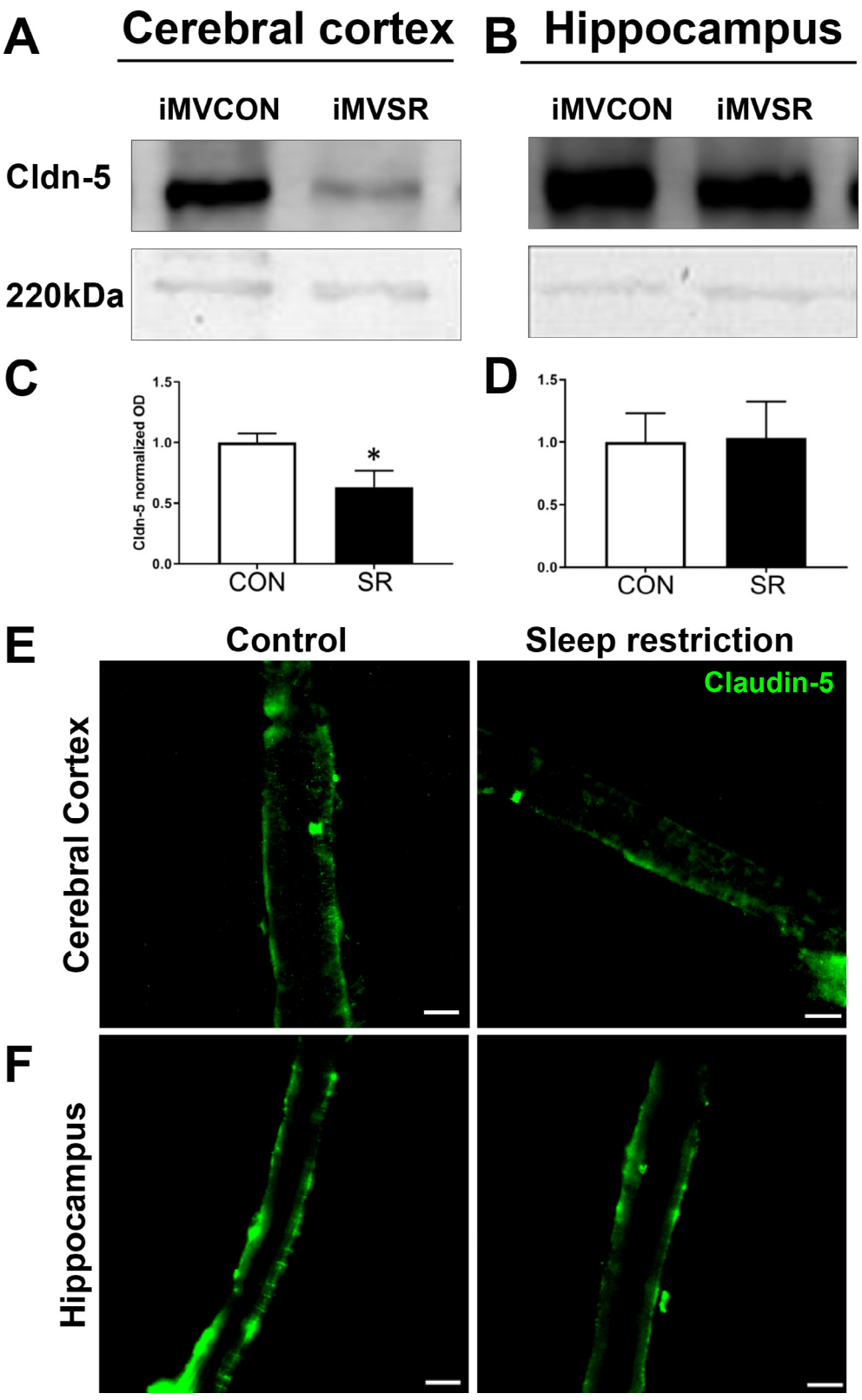

Fig. 9. Chronic sleep restriction reduces claudin-5 protein expression in isolated brain microvessels. Representative Western blot showing claudin-5 expression in isolated microvessels (iMV) from intact control (CON) and sleep restricted (SR) groups (A, B). Normalized levels of claudin-5 expression in the iMV of the cerebral cortex (C) and hippocampus (D) were obtained using a band of 220 kDa marked with Ponceau red. Samples were analyzed by duplicate in separate PVDF membranes. Mean ± standard error of the mean. *$p < 0.01$ as compared to the CON group. Immunofluorescent staining for claudin-5 in iMV from cerebral cortex (E) and hippocampus (F) of CON and SR groups. Note in the iMV from cerebral cortex (E) the linear expression of claudin-5 along the capillary in the CON group and the loss of this staining pattern in the iMV from the SR group. Scale bar: 20 μm.

levels of the adenosine-synthesizing ectonucleotidase, CD73, remained without changes between control ($p = 0.6341$) and sleep-restricted rats ($p = 0.7151$) (Fig. 12).

4. Discussion

Given the important role of pericytes in the maintenance of the barrier properties of the blood-brain barrier (Duz et al., 2007; Nakagawa et al., 2009; Bell et al., 2010; Rustenhoven et al., 2017), this study aimed to evaluate the changes in pericyte-brain endothelial cell interactions during sleep loss, and tried to characterize the effects of pericyte detachment in blood-brain barrier physiology in sleep-restricted rats. Here, we found that sleep loss promotes pericyte detachment from the capillary wall as indicated by the significant reduction in

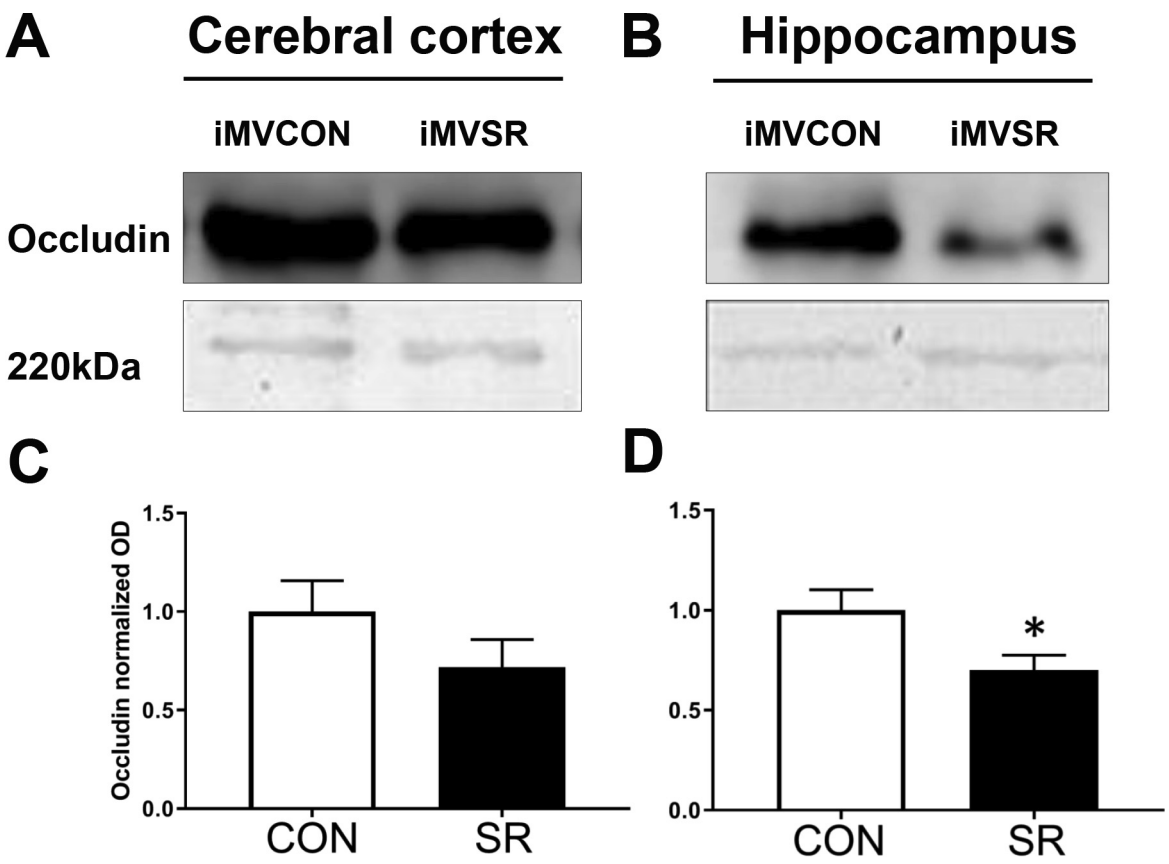

Fig. 10. Chronic sleep restriction reduces occludin protein expression in isolated brain microvessels. A, B) Representative Western blot showing occludin protein expression in isolated microvessels (iMV) from intact control (CON) and sleep restricted (SR) groups. C, D) Normalized levels of occludin expression in the iMV of the cerebral cortex and hippocampus were obtained using a band of 220 kDa marked with Ponceau red. Samples were analyzed by duplicate in separate PVDF membranes. Mean ± standard error of the mean. *p < 0.01 as compared to the CON group.

the expression of PDGFR-β, a marker of pericytes amply used to study pericyte coverage of brain microvessels (Winkler et al., 2010). PDGFR-β role in maintaining the barrier phenotype in brain endothelial cells has been clearly established in the $Pdgfb^{ret/ret}$ mutant mice, a model in which PDGF-B presents a truncating mutation and pericytes are partially dissociated from brain endothelial cells. $Pdgfb^{ret/ret}$ mice present endothelial cell membrane protrusions into the vessel lumen, increased number of cytoplasmic vesicles and increased blood-brain barrier permeability to circulating tracers, such as Evans blue (Daneman et al., 2010). We observed similar changes in the phenotype of brain endothelial cells in sleep-restricted rats. For instance, sleep loss increased blood-brain barrier permeability to Evans blue and fluorescein along with increased number of cytoplasmic vesicles and cytoplasmic protrusions into the vessel lumen in hippocampal endothelial cells (Gomez-Gonzalez et al., 2013; Hurtado-Alvarado et al., 2017). The present data are in concordance with our previous findings indicating that PDGFR-β reduction induces pericyte loss and compromises the blood-brain barrier integrity.

In addition to reduced expression of PDGFR-β, we found that isolated MVs from the sleep-restricted rats exhibit round shaped cells close to the capillary wall, again indicating pericyte detachment from the capillary wall. Another evidence of pericyte-endothelial cell detachment is the reduction of connexin 43 in isolated brain microvessels from the cerebral cortex of sleep restricted rats. Connexin 43 is the major connexin expressed in the central nervous system (Figueroa and Duling, 2009) and the decreased expression of connexin 43 may compromise pericyte functionality at the early stages of diabetic retinopathy, ensuing poor vasomotor control in diabetic retina (Ivanova et al., 2017). In addition, during chronic diabetes the loss of signaling between vascular cells due to connexin 43 downregulation, leads to apoptosis of vascular cells in the mammalian retina (Bobbie et al., 2010). In our case, pericyte detachment from the capillary wall was not concurrent with apoptosis, as depicted by the normal active caspase-3 expression observed in the isolated MVs from the cerebral cortex and hippocampus of sleep restricted rats as compared to the intact controls. Our data suggest that connexin 43 plays an important role regulating pericyte-endothelial cell interactions and its downregulation could contribute to blood-brain barrier defects in sleep-restricted rats.

As expected, the reduction in the pericyte coverage of brain microvessels was concurrent with an increased blood-brain barrier permeability to low- and high- molecular weight tracers as well as to rhodamine-123, a substrate of efflux pumps. The increased blood-brain barrier permeability to rhodamine 123 points to a change in P-glycoprotein functionality in isolated brain MVs from cerebral cortex and hippocampus in the sleep restricted rats. P-glycoprotein is the main efflux transporter expressed in brain endothelial cells and its dysfunction increases the accumulation of toxic molecules in the brain parenchyma (Kamiie et al., 2008). The function of P-glycoprotein was enhanced in co-cultures of endothelial cells with pericytes, indicating that pericytes influence this barrier property (Nakagawa et al., 2009; Vandenhaute et al., 2011). By the contrary, the upregulation of proinflammatory cytokines leads to P-glycoprotein transport dysfunction (Ho and Piquette-Miller, 2006). Rats injected with *Klebsiella pneumoniae* endotoxin presented a reduced biliary, renal, and tubular secretory clearances of rhodamine 123 indicating an impairment of P-glycoprotein transport; and the effects were related to increased levels of TNF-α in plasma (Ando et al., 2001). In addition, rats treated with lipopolysaccharide, which increases the expression of TNF-α, IL-β and IL-6, presented a down-regulation of P-glycoprotein function as depicted by the accumulation of ^{3}H-digoxin in the brain; again indicating that

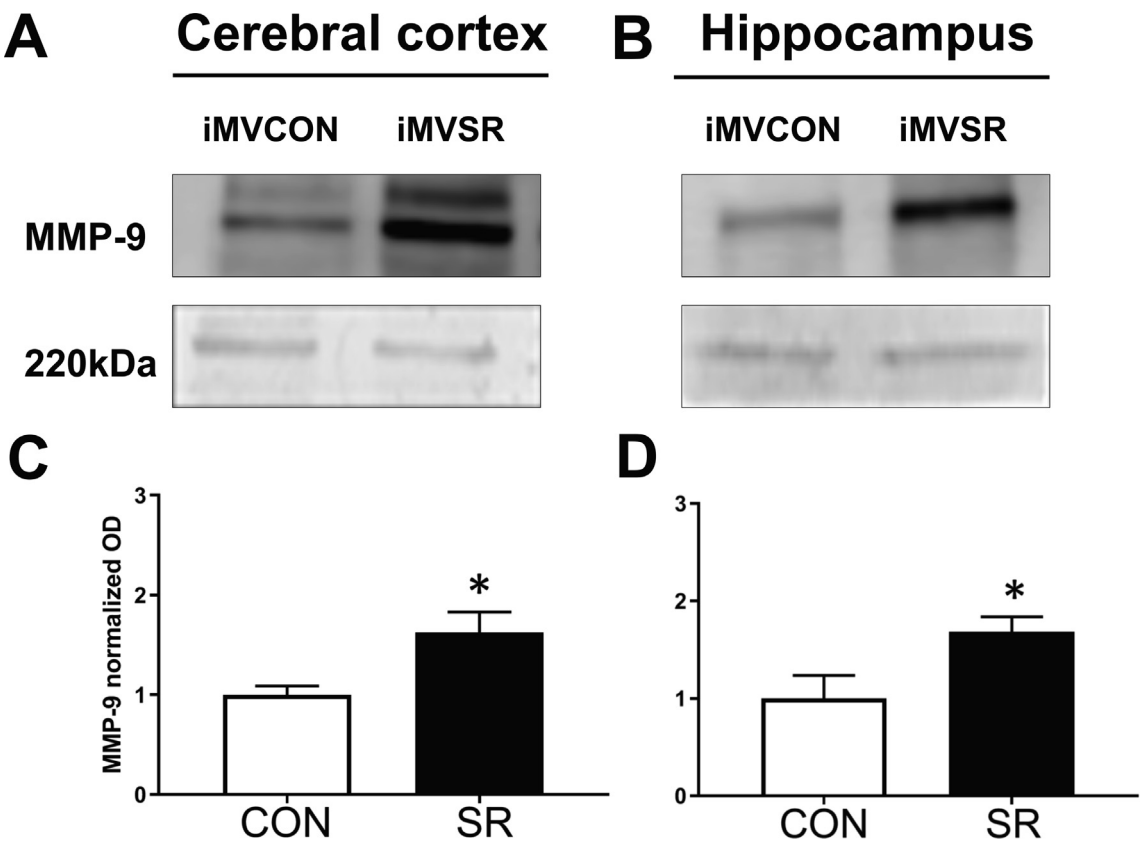

Fig. 11. Chronic sleep restriction increases MMP-9 expression in isolated brain microvessels from the cerebral cortex and hippocampus. Representative Western blot images of isolated brain microvessels (iMV) show a significant increase in the expression of MMP-9 in cerebral cortex (A) and hippocampus (B) after 10 days of sleep restriction (SR) in comparison with the control group (CON). C, D) Graphs depict the expression levels of MMP-9 using a band of 220 KDa marked with Ponceau red for normalization. Samples were analyzed by duplicate in separate PVDF membranes. Mean ± standard error of the mean. *p < 0.01 as compared to the CON group.

inflammation modulates P-glycoprotein function (Goralski et al., 2003; Uchida et al., 2014).

Here we also found blood-brain barrier hyperpermeability to small- and large-molecular weight tracers in the cerebral cortex and hippocampus. Similar changes in blood-brain barrier permeability have been found after 6-day sleep loss in C57/BL6 mice (He et al., 2014); and after 10-day sleep restriction in both Wistar rats (Gomez-Gonzalez et al., 2013; Hurtado-Alvarado et al., 2017) and C57/BL6 mice (Hurtado-Alvarado et al., 2018). Those permeability changes occurred simultaneously with decreased tight junction protein expression in the sleep restricted rats, both in the present experiment and in previously published papers (Hurtado-Alvarado et al., 2017, 2018). Indeed, increased blood-brain barrier permeability secondary to pericyte loss associates with a down-regulation of claudin-5, occludin and the scaffold protein ZO-1 (Armulik et al., 2010; Villaseñor et al., 2017). These results highlight the importance of intercellular interactions to maintain blood-brain barrier properties.

The reduced expression of the tight junction proteins was related with an overexpression of MMP-9 in isolated MVs from cerebral cortex and hippocampus. Under neuropathological conditions, such as cerebral ischemia, the pericyte detaches from the capillary wall and acquires proteolytic activity (Dave et al., 2018); indeed, previous evidence indicates that the pericyte becomes the principal cell releasing MMP-9 as compared with astrocytes, microglia, and neurons (Takata et al., 2011). Although we did not evaluate in our isolated brain MVs which cellular type is producing and releasing MMP-9, we propose that in sleep-restricted rats the detachment of pericytes from the capillary wall is accompanied by a change in their morphology that will drive the release of endopeptidases, like MMP-9, contributing to the degradation of the basal lamina. Those effects, pericyte transformation and its acquisition of proteolytic activity, may be related with the low-grade inflammatory environment at the central nervous system, as previously observed in other animal models with inflammation, such as in lipopolysaccharide treated mice (Nishioku et al., 2009).

It is known that neuroinflammation is one of the causes of blood-brain barrier dysfunction in many diseases and one of the signaling pathways involved is the activation of the transcription factor NFκB. Interestingly, increased expression of phosphorylated NFκB was observed only in cerebral cortex, which correlates with the decreased expression of claudin-5 protein in sleep-restricted rats. Chiu and Lai (2013) described in a model of eosinophilic meningoencephalitis an increase in the levels of p-NFκB that correlated with decreased claudin-5 expression and increased blood-brain barrier permeability to Evans blue. In the case of the hippocampus, there was an increased expression of the A_{2A} adenosine receptor in sleep-restricted rats. This result is consistent with our previously reported experiments in which sleep restriction increased A_{2A} receptor expression in the hippocampus and basal nuclei but not in the cerebral cortex (Hurtado-Alvarado et al., 2016a). *In vitro* studies have reported that A_{2A} stimulation decreases TEER values and increases blood-brain barrier permeability to chemotherapeutic drugs and T cells (Dunwiddie and Masino, 2001; Kim and Bynoe, 2015). Moreover, Kim et al. (2012) reported that sleep deprivation increased mRNA levels of A_{2A} adenosine receptor in the hippocampus but no in other brain regions. Together, these findings suggest that A_{2A} adenosine receptor performs a regulatory role in blood-brain barrier physiology, which may depend on its distribution and expression in each brain region.

Although sleep loss altered pericyte-brain endothelial cell

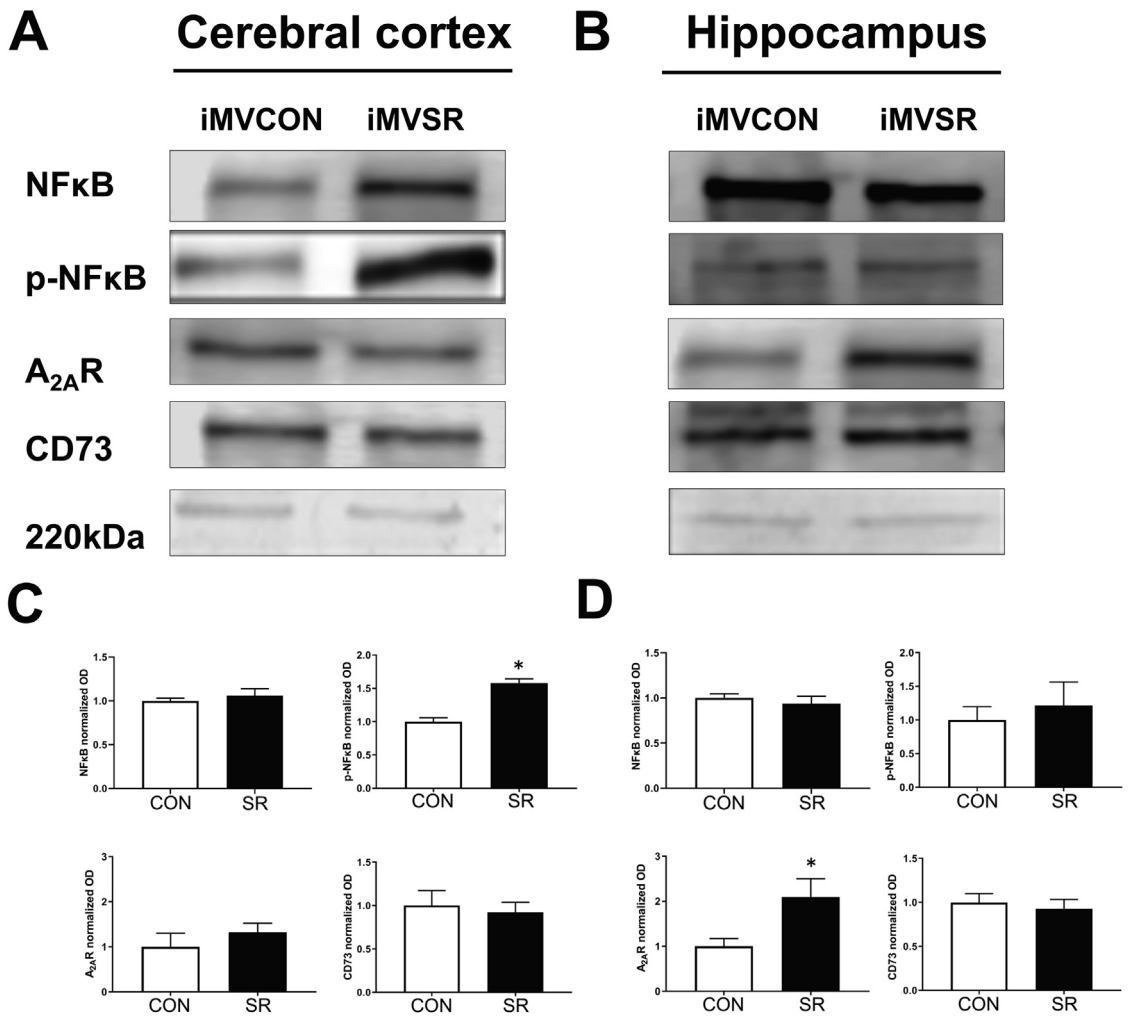

Fig. 12. Chronic sleep restriction modulates the expression of pro-inflammatory mediators in isolated microvessels from the cerebral cortex and hippocampus. Representative Western blot of isolated microvessels (iMV) from control (CON) and sleep restricted (SR) groups (A, B). Graphs depict the expression levels of NFκB, p-NFκB, A_{2A} adenosine receptor and CD73 in iMV from the cerebral cortex (C) and hippocampus (D) of CON and SR groups. The expression levels of the proteins of interests were normalized using a band of 220 KDa marked with red Ponceau. Quantification was performed by duplicate for each sample. Mean ± standard error of the mean. *$p < 0.01$ as compared to the CON group.

interactions, there was no change in metabolic activity of brain endothelial cells, as depicted by absence of changes in the expression of the primary glucose transporter at the level of the blood-brain barrier, GLUT-1, and the normal mitochondrial respiratory control. Our results differ from previously published studies, He et al. (2014) shown a downregulation of GLUT-1 expression in 6-day sleep restricted C57/Bl6 mice and Petit et al. (2010) found increased levels of GLUT-1 mRNA after 6 h of sleep deprivation in mice. These discrepancies may be due to the different techniques used to induce sleep loss, as well as the time the animals were in this condition. The absence of change in mitochondrial respiratory control between sleep-restricted and intact control groups indicates a preserved functional coupling of respiration and ATP synthesis in the mitochondria of isolated brain MVs despite sleep loss. Our findings suggest that 10 days of sleep loss does not compromise the metabolic activity of the vascular cells.

Such large changes in pericyte phenotype may be a consequence of direct effects of sleep loss on pericyte physiology, besides to be regulated by local inflammatory mediators released by resident cells (eg. astroglia and microglia). Indeed, Nakazato et al. (2017) found that the knock down of the circadian clock gene *bmal1* increased blood-brain barrier permeability to Evans blue by selectively downregulating the expression of the PDGFR-β in brain pericytes. As sleep loss has been shown to reduce DNA binding of brain and muscle ARNT-like 1 (BMAL1) protein to the promotor regions of target genes (eg. *per2* and other clock genes) in the cerebral cortex (Mongrain et al., 2011), it is highly possible that sleep loss may be altering the circadian clock gene loop and as a consequence might be preventing BMAL1 binding to the DNA promotor sequence in the *pdgfr-β* gene, ensuing poor PDGFR-β expression.

According to our findings in this study, we propose that during sleep loss the pericyte changes its phenotype and may acquire proteolytic functions by releasing proteolytic enzymes, as result of an inflammatory status mediated by the activation of the transcription factor NFκB in cerebral cortex, and A_{2A} adenosine receptor upregulation in the hippocampus. The different signaling pathways used by both regions suggest a heterogeneity of pathways that regulate pericyte-endothelial cell interactions during pathological conditions. Our study provides the possibility of considering different mechanisms by which sleep loss can be related to the development or exacerbation of neurodegenerative diseases such as Alzheimer's, ischemia, epilepsy and stroke, where the interactions between pericytes/endothelial cells and neuroinflammation seem to have a key role.

5. Conclusion

Chronic sleep restriction decreases the interactions between brain endothelial cells and pericytes by decreasing the expression of the proteins that maintain the junctions between them, such as PDGFR-β and connexin 43. The loss of pericyte-endothelial cell interactions concurs with a disruption of the barrier properties by reducing tight junction proteins between endothelial cells and increasing blood-brain barrier permeability to exogenous tracers in sleep-restricted rats. The impairment in the cellular interactions between pericytes and endothelial cells seem to depend on a low-grade inflammatory status after chronic sleep restriction.

Funding

This work was partially supported by the Universidad Autónoma Metropolitana to BGG. The funding sources had no role in study design; in the collection, analysis and interpretation of data; in the writing of the report; and in the decision to submit the article for publication.

Declaration of Competing Interest

None.

Acknowledgment

to Dr. Óscar Flores Herrera from Dept. Biochemistry, Medicine School, Universidad Nacional Autónoma de México, for the technical support in the oximetry experiments. To MS. María Cristina Acosta García from the Electron Microscopy Lab, Dept. Biology of Reproduction, Biological Science Division of the Universidad Autónoma Metropolitana, Unidad Iztapalapa for their technical support with the scanning electron microscopy experiments.

Appendix A. Supplementary data

Supplementary data to this article can be found online at https://doi.org/10.1016/j.bbi.2020.05.077.

References

Ando, H., Nishio, Y., Ito, K., Nakao, A., Wang, L., Zhao, Y.L., et al., 2001. Effect of endotoxin on P-glycoprotein-mediated biliary and renal excretion of rhodamine-123 in rats. Antimicrob. Agents Chemother. 45 (12), 3462–3467. https://doi.org/10.1128/AAC.45.12.3462-3467.2001.

Arango-Lievano, M., Boussadia, B., De Terdonck, L.D.T., Gault, C., Fontanaud, P., Lafont, C., et al., 2018. Topographic reorganization of cerebrovascular mural cells under seizure conditions. Cell Rep. 23 (4), 1045–1059. https://doi.org/10.1016/j.celrep.2018.03.110.

Armulik, A., Abramsson, A., Betsholtz, C., 2005. Endothelial/pericyte interactions. Circ. Res. 97 (6), 512–523. https://doi.org/10.1161/01.RES.0000182903.16652.d7.

Armulik, A., Genové, G., Betsholtz, C., 2011. Pericytes: developmental, physiological, and pathological perspectives, problems, and promises. Dev. Cell 21 (2), 193–215. https://doi.org/10.1016/j.devcel.2011.07.001.

Armulik, A., Genové, G., Mäe, M., Nisancioglu, M.H., Wallgard, E., Niaudet, C., et al., 2010. Pericytes regulate the blood–brain barrier. Nature 468 (7323), 557–561. https://doi.org/10.1038/nature09522.

Bell, R.D., Winkler, E.A., Sagare, A.P., Singh, I., LaRue, B., Deane, R., Zlokovic, B.V., 2010. Pericytes control key neurovascular functions and neuronal phenotype in the adult brain and during brain aging. Neuron 68 (3), 409–427. https://doi.org/10.1016/j.neuron.2010.09.043.

Benjamin, L.E., Hemo, I., Keshet, E., 1998. A plasticity window for blood vessel remodelling is defined by pericyte coverage of the preformed endothelial network and is regulated by PDGF-B and VEGF. Development 125 (9), 1591.

Bobbie, M.W., Roy, S., Trudeau, K., Munger, S.J., Simon, A.M., Roy, S., 2010. Reduced connexin 43 expression and its effect on the development of vascular lesions in retinas of diabetic mice. Invest. Opthalmol. Visual Sci. 51 (7), 3758. https://doi.org/10.1167/iovs.09-4489.

Chiu, P.-S., Lai, S.-C., 2013. Matrix metalloproteinase-9 leads to claudin-5 degradation via the NF-κB pathway in BALB/c mice with eosinophilic meningoencephalitis caused by Angiostrongylus cantonensis. PLoS One 8 (3), e53370. https://doi.org/10.1371/journal.pone.0053370.

Daneman, R., Zhou, L., Kebede, A.A., Barres, B.A., 2010. Pericytes are required for blood–brain barrier integrity during embryogenesis. Nature 468 (7323), 562–566. https://doi.org/10.1038/nature09513.

Dave, J.M., Mirabella, T., Weatherbee, S.D., Greif, D.M., 2018. Pericyte ALK5/TIMP3 axis contributes to endothelial morphogenesis in the developing brain. Dev. Cell 44 (6), 665–678.e6. https://doi.org/10.1016/j.devcel.2018.01.018.

Dunwiddie, T.V., Masino, S.A., 2001. The role and regulation of adenosine in the central nervous system. Annu. Rev. Neurosci. 24 (1), 31–55. https://doi.org/10.1146/annurev.neuro.24.1.31.

Duz, B., Oztas, E., Erginay, T., Erdogan, E., Gonul, E., 2007. The effect of moderate hypothermia in acute ischemic stroke on pericyte migration: an ultrastructural study. Cryobiology 55 (3), 279–284. https://doi.org/10.1016/j.cryobiol.2007.08.009.

Figueroa, X.F., Duling, B.R., 2009. Gap junctions in the control of vascular function. Antioxid. Redox Signal. 11 (2), 251–266. https://doi.org/10.1089/ars.2008.2117.

Fujimoto, K., 1995. Pericyte-endothelial gap junctions in developing rat cerebral capillaries: a fine structural study. Anatom. Rec. 242 (4), 562–565. https://doi.org/10.1002/ar.1092420412.

Gomez-Gonzalez, B., Hurtado-Alvarado, G., Esqueda-Leon, E., Santana- Miranda, R., Rojas-Zamorano, J., Velazquez-Moctezuma, J., 2013. REM sleep loss and recovery regulates blood-brain barrier function. Curr. Neurovasc. Res. 10 (3), 197–207. https://doi.org/10.2174/15672026113109990002.

Goralski, K.B., Hartmann, G., Piquette-Miller, M., Renton, K.W., 2003. Downregulation of *mdr1a* expression in the brain and liver during CNS inflammation alters the *in vivo* disposition of digoxin. Br. J. Pharmacol. 139 (1), 35–48. https://doi.org/10.1038/sj.bjp.0705227.

Hall, C.N., Reynell, C., Gesslein, B., Hamilton, N.B., Mishra, A., Sutherland, B.A., Attwell, D., 2014. Capillary pericytes regulate cerebral blood flow in health and disease. Nature 508 (7494), 55–60. https://doi.org/10.1038/nature13165.

Hayashi, K., Nakao, S., Nakaoke, R., Nakagawa, S., Kitagawa, N., Niwa, M., 2004. Effects of hypoxia on endothelial/pericytic co-culture model of the blood–brain barrier. Regul. Pept. 123 (1–3), 77–83. https://doi.org/10.1016/j.regpep.2004.05.023.

He, J., Hsuchou, H., He, Y., Kastin, A.J., Wang, Y., Pan, W., 2014. Sleep restriction impairs blood-brain barrier function. J. Neurosci. 34 (44), 14697–14706. https://doi.org/10.1523/JNEUROSCI.2111-14.2014.

Ho, E., Piquette-Miller, M., 2006. Regulation of multidrug resistance by pro-inflammatory cytokines. Curr. Cancer Drug Targets 6 (4), 295–311. https://doi.org/10.2174/156800906777441753.

Hurtado-Alvarado, G., Becerril-Villanueva, E., Contis-Montes de Oca, A., Domínguez-Salazar, E., Salinas-Jazmín, N., Pérez-Tapia, S.M., et al., 2018. The yin/yang of inflammatory status: blood-brain barrier regulation during sleep. Brain Behav. Immun. 69, 154–166. https://doi.org/10.1016/j.bbi.2017.11.009.

Hurtado-Alvarado, G., Velázquez-Moctezuma, J., Gómez-González, B., 2017. Chronic sleep restriction disrupts interendothelial junctions in the hippocampus and increases blood-brain barrier permeability: chronic sleep restriction disrupts interendothelial junctions. J. Microsc. 268 (1), 28–38. https://doi.org/10.1111/jmi.12583.

Hurtado-Alvarado, Gabriela, Domínguez-Salazar, E., Velázquez-Moctezuma, J., Gómez-González, B., 2016a. A2A adenosine receptor antagonism reverts the blood-brain barrier dysfunction induced by sleep restriction. PLoS One 11 (11), e0167236. https://doi.org/10.1371/journal.pone.0167236.

Hurtado-Alvarado, G., Domínguez-Salazar, E., Pavon, L., Velázquez-Moctezuma, J., Gómez-González, B., 2016b. Blood-brain barrier disruption induced by chronic sleep loss: low-grade inflammation may be the link. J. Immunol. Res. 2016, 4576012. https://doi.org/10.1155/2016/4576012.

Ivanova, E., Kovacs-Oller, T., Sagdullaev, B.T., 2017. Vascular pericyte impairment and connexin 43 gap junction deficit contribute to vasomotor decline in diabetic retinopathy. J. Neurosci. 37 (32), 7580–7594. https://doi.org/10.1523/JNEUROSCI.0187-17.2017.

Kamiie, J., Ohtsuki, S., Iwase, R., Ohmine, K., Katsukura, Y., Yanai, K., et al., 2008. Quantitative atlas of membrane transporter proteins: development and application of a highly sensitive simultaneous LC/MS/MS method combined with novel in-silico peptide selection criteria. Pharm. Res. 25 (6), 1469–1483. https://doi.org/10.1007/s11095-008-9532-4.

Kim, D.-G., Bynoe, M.S., 2015. A2A adenosine receptor regulates the human blood-brain barrier permeability. Mol. Neurobiol. 52 (1), 664–678. https://doi.org/10.1007/s12035-014-8879-2.

Kim, Y., Bolortuya, Y., Chen, L., Basheer, R., McCarley, R.W., Strecker, R.E., 2012. Decoupling of sleepiness from sleep time and intensity during chronic sleep restriction: evidence for a role of the adenosine system. Sleep 35 (6), 861–869. https://doi.org/10.5665/sleep.1890.

Lebrin, F., Srun, S., Raymond, K., Martin, S., van den Brink, S., Freitas, C., et al., 2010. Thalidomide stimulates vessel maturation and reduces epistaxis in individuals with hereditary hemorrhagic telangiectasia. Nat. Med. 16 (4), 420–428. https://doi.org/10.1038/nm.2131.

Leveen, P., Pekny, M., Gebre-Medhin, S., Swolin, B., Larsson, E., Betsholtz, C., 1994. Mice deficient for PDGF B show renal, cardiovascular, and hematological abnormalities. Genes Dev. 8 (16), 1875–1887. https://doi.org/10.1101/gad.8.16.1875.

Manchanda, S., Singh, H., Kaur, T., Kaur, G., 2018. Low-grade neuroinflammation due to chronic sleep deprivation results in anxiety and learning and memory impairments. Mol. Cell. Biochem. 449 (1–2), 63–72. https://doi.org/10.1007/s11010-018-3343-7.

Mongrain, V., La Spada, F., Curie, T., Franken, P., 2011. Sleep loss reduces the DNA-binding of BMAL1, CLOCK, and NPAS2 to specific clock genes in the mouse cerebral cortex. PLoS One 6 (10), e26622. https://doi.org/10.1371/journal.pone.0026622.

Nakagawa, S., Deli, M.A., Kawaguchi, H., Shimizudani, T., Shimono, T., Kittel, Á., Niwa, M., 2009. A new blood–brain barrier model using primary rat brain endothelial cells, pericytes and astrocytes. Neurochem. Int. 54 (3–4), 253–263. https://doi.org/10.1016/j.neuint.2008.12.002.

Nakazato, R., Kawabe, K., Yamada, D., Ikeno, S., Mieda, M., Shimba, S., Hinoi, E., Yoneda,

Y., Takarada, T., 2017. Disruption of bmal1 impairs blood-brain barrier integrity via pericyte dysfunction. J. Neurosci. 37 (42), 10052–10062. https://doi.org/10.1523/JNEUROSCI.3639-16.2017.

Neuhaus, A.A., Couch, Y., Sutherland, B.A., Buchan, A.M., 2017. Novel method to study pericyte contractility and responses to ischaemia *in vitro* using electrical impedance. J. Cereb. Blood Flow Metab. 37 (6), 2013–2024. https://doi.org/10.1177/0271678X16659495.

Nishioku, T., Dohgu, S., Takata, F., Eto, T., Ishikawa, N., Kodama, K.B., et al., 2009. Detachment of brain pericytes from the basal lamina is involved in disruption of the blood-brain barrier caused by lipopolysaccharide-induced sepsis in mice. Cell. Mol. Neurobiol. 29 (3), 309–316. https://doi.org/10.1007/s10571-008-9322-x.

Petit, J.-M., Tobler, I., Kopp, C., Morgenthaler, F., Borbély, A.A., Magistretti, P.J., 2010. Metabolic response of the cerebral cortex following gentle sleep deprivation and modafinil administration. Sleep 33 (7), 901–908. https://doi.org/10.1093/sleep/33.7.901.

Rustenhoven, J., Jansson, D., Smyth, L.C., Dragunow, M., 2017. Brain pericytes as mediators of neuroinflammation. Trends Pharmacol. Sci. 38 (3), 291–304. https://doi.org/10.1016/j.tips.2016.12.001.

Shimizu, F., Sano, Y., Maeda, T., Abe, M., Nakayama, H., Takahashi, R., et al., 2008. Peripheral nerve pericytes originating from the blood-nerve barrier expresses tight junctional molecules and transporters as barrier-forming cells. J. Cell. Physiol. 217 (2), 388–399. https://doi.org/10.1002/jcp.21508.

Stark, K., Eckart, A., Haidari, S., Tirniceriu, A., Lorenz, M., von Brühl, M.-L., et al., 2013. Capillary and arteriolar pericytes attract innate leukocytes exiting through venules and “instruct” them with pattern-recognition and motility programs. Nat. Immunol. 14 (1), 41–51. https://doi.org/10.1038/ni.2477.

Takata, F., Dohgu, S., Matsumoto, J., Takahashi, H., Machida, T., Wakigawa, T., et al., 2011. Brain pericytes among cells constituting the blood-brain barrier are highly sensitive to tumor necrosis factor-α, releasing matrix metalloproteinase-9 and migrating in vitro. J. Neuroinflamm. 8 (1), 106. https://doi.org/10.1186/1742-2094-8-106.

Tarallo, S., Beltramo, E., Berrone, E., Porta, M., 2012. Human pericyte–endothelial cell interactions in co-culture models mimicking the diabetic retinal microvascular environment. Acta Diabetol. 49 (S1), 141–151. https://doi.org/10.1007/s00592-012-0390-5.

Uchida, Y., Ohtsuki, S., Terasaki, T., 2014. Pharmacoproteomics-based reconstruction of in vivo P-glycoprotein function at blood-brain barrier and brain distribution of substrate verapamil in pentylenetetrazole-kindled epilepsy, spontaneous epilepsy, and phenytoin treatment models. Drug Metab. Dispos. 42 (10), 1719–1726. https://doi.org/10.1124/dmd.114.059055.

Vandenhaute, E., Dehouck, L., Boucau, M.-C., Sevin, E., Uzbekov, R., Tardivel, M., et al., 2011. Modelling the neurovascular unit and the blood-brain barrier with the unique function of pericytes. Curr. Neurovasc. Res. 8 (4), 258–269. https://doi.org/10.2174/156720211798121016.

Vates, G.E., Takano, T., Zlokovic, B., Nedergaard, M., 2010. Pericyte constriction after stroke: the jury is still out. Nat. Med. 16 (9). https://doi.org/10.1038/nm0910-959. 959–959.

Villaseñor, R., Kuennecke, B., Ozmen, L., Ammann, M., Kugler, C., Grüninger, F., et al., 2017. Region-specific permeability of the blood–brain barrier upon pericyte loss. J. Cereb. Blood Flow Metab. 37 (12), 3683–3694. https://doi.org/10.1177/0271678X17697340.

Winkler, E.A., Bell, R.D., Zlokovic, B.V., 2010. Pericyte-specific expression of PDGF beta receptor in mouse models with normal and deficient PDGF beta receptor signaling. Mol. Neurodegener. 5 (1), 32. https://doi.org/10.1186/1750-1326-5-32.

Wisniewska-Kruk, J., Hoeben, K.A., Vogels, I.M.C., Gaillard, P.J., Van Noorden, C.J.F., Schlingemann, R.O., Klaassen, I., 2012. A novel co-culture model of the blood-retinal barrier based on primary retinal endothelial cells, pericytes and astrocytes. Exp. Eye Res. 96 (1), 181–190. https://doi.org/10.1016/j.exer.2011.12.003.